Biomedical Optics EXPRESS

Detection of single fluorescent proteins inside eukaryotic cells using two-photon fluorescence

Ximiao Hou and Wei Cheng*

Department of Pharmaceutical Sciences, University of Michigan, 428 Church Street, Ann Arbor, Michigan 48109, USA

**chengwe@umich.edu*

Abstract: Imaging single fluorescent proteins in a live cell is a challenging task because of the strong cellular autofluorescence. Autofluorescence can be minimized by reducing fluorescence excitation volume. Total internal reflection fluorescence (TIRF) microscopy has been routinely used to reduce excitation volume and detect single protein molecules in or close to cell membrane. However, the limited penetration depth of evanescent field excludes imaging of single fluorescent proteins that reside deep inside a eukaryotic cell. Here we report detection of single fluorescent proteins inside eukaryotic cells by two-photon fluorescence (TPF) microscopy. TPF has an excitation volume less than 0.1 femtoliter (fL). Cell autofluorescence under TPF is low and thus enables us to detect single enhanced green fluorescent proteins (EGFP) and single monomeric teal fluorescent proteins (mTFP1.0) that reside several microns deep inside the cell. Discrete stepwise photobleaching of TPF was observed for both proteins inside the cell. Quantitative analysis of single-molecule fluorescence trajectories show that mTFP1.0 is about twofold brighter than EGFP, while its fluorescence on-time before bleaching is about 10 fold shorter. These findings demonstrate the sensitivity of TPF for imaging of eukaryotic cells at single-molecule level and will be useful for measurement of protein stoichiometry inside the cell.

OCIS codes: (190.4180) Multiphoton processes; (170.1530) Cell analysis; (170.2520) Fluorescence microscopy.

References and links

1. G. W. Li and X. S. Xie, "Central dogma at the single-molecule level in living cells," Nature **475**(7356), 308–315 (2011).
2. T. Ha, I. Rasnik, W. Cheng, H. P. Babcock, G. H. Gauss, T. M. Lohman, and S. Chu, "Initiation and re-initiation of DNA unwinding by the *Escherichia coli* Rep helicase," Nature **419**(6907), 638–641 (2002).
3. E. Toprak and P. R. Selvin, "New fluorescent tools for watching nanometer-scale conformational changes of single molecules," Annu. Rev. Biophys. Biomol. Struct. **36**(1), 349–369 (2007).
4. N. C. Shaner, P. A. Steinbach, and R. Y. Tsien, "A guide to choosing fluorescent proteins," Nat. Methods **2**(12), 905–909 (2005).
5. D. Axelrod, T. P. Burghardt, and N. L. Thompson, "Total internal reflection fluorescence," Annu. Rev. Biophys. Bioeng. **13**(1), 247–268 (1984).
6. J. G. Ritter, R. Veith, A. Veenendaal, J. P. Siebrasse, and U. Kubitscheck, "Light sheet microscopy for single molecule tracking in living tissue," PLoS ONE **5**(7), e11639 (2010).
7. T. A. Planchon, L. Gao, D. E. Milkie, M. W. Davidson, J. A. Galbraith, C. G. Galbraith, and E. Betzig, "Rapid three-dimensional isotropic imaging of living cells using Bessel beam plane illumination," Nat. Methods **8**(5), 417–423 (2011).
8. F. Cella Zanacchi, Z. Lavagnino, M. Perrone Donnorso, A. Del Bue, L. Furia, M. Faretta, and A. Diaspro, "Live-cell 3D super-resolution imaging in thick biological samples," Nat. Methods **8**(12), 1047–1049 (2011).

#157703 - $15.00 USD Received 7 Nov 2011; revised 15 Jan 2012; accepted 15 Jan 2012; published 18 Jan 2012

9. W. Denk, J. H. Strickler, and W. W. Webb, "Two-photon laser scanning fluorescence microscopy," Science **248**(4951), 73–76 (1990).
10. E. J. Sánchez, L. Novotny, G. R. Holtom, and X. S. Xie, "Room-temperature fluorescence imaging and spectroscopy of single molecules by two-photon excitation," J. Phys. Chem. A **101**(38), 7019–7023 (1997).
11. J. T. Groves, R. Parthasarathy, and M. B. Forstner, "Fluorescence imaging of membrane dynamics," Annu. Rev. Biomed. Eng. **10**(1), 311–338 (2008).
12. P. D. Simonson, H. A. Deberg, P. Ge, J. K. Alexander, O. Jeyifous, W. N. Green, and P. R. Selvin, "Counting bungarotoxin binding sites of nicotinic acetylcholine receptors in mammalian cells with high signal/noise ratios," Biophys. J. **99**(10), L81–L83 (2010).
13. W. Ji, P. Xu, Z. Li, J. Lu, L. Liu, Y. Zhan, Y. Chen, B. Hille, T. Xu, and L. Chen, "Functional stoichiometry of the unitary calcium-release-activated calcium channel," Proc. Natl. Acad. Sci. U.S.A. **105**(36), 13668–13673 (2008).
14. M. C. Leake, J. H. Chandler, G. H. Wadhams, F. Bai, R. M. Berry, and J. P. Armitage, "Stoichiometry and turnover in single, functioning membrane protein complexes," Nature **443**(7109), 355–358 (2006).
15. M. H. Ulbrich and E. Y. Isacoff, "Subunit counting in membrane-bound proteins," Nat. Methods **4**(4), 319–321 (2007).
16. S. C. Kohout, M. H. Ulbrich, S. C. Bell, and E. Y. Isacoff, "Subunit organization and functional transitions in Ci-VSP," Nat. Struct. Mol. Biol. **15**(1), 106–108 (2008).
17. W. Kaiser and C. G. B. Garrett, "2-Photon excitation in Caf^{2}–Eu^{2+}," Phys. Rev. Lett. **7**(6), 229–231 (1961).
18. W. R. Zipfel, R. M. Williams, and W. W. Webb, "Nonlinear magic: multiphoton microscopy in the biosciences," Nat. Biotechnol. **21**(11), 1369–1377 (2003).
19. J. M. Squirrell, D. L. Wokosin, J. G. White, and B. D. Bavister, "Long-term two-photon fluorescence imaging of mammalian embryos without compromising viability," Nat. Biotechnol. **17**(8), 763–767 (1999).
20. K. Svoboda and R. Yasuda, "Principles of two-photon excitation microscopy and its applications to neuroscience," Neuron **50**(6), 823–839 (2006).
21. F. Helmchen and W. Denk, "Deep tissue two-photon microscopy," Nat. Methods **2**(12), 932–940 (2005).
22. M. D. Cahalan and I. Parker, "Choreography of cell motility and interaction dynamics imaged by two-photon microscopy in lymphoid organs," Annu. Rev. Immunol. **26**(1), 585–626 (2008).
23. P. T. So, C. Y. Dong, B. R. Masters, and K. M. Berland, "Two-photon excitation fluorescence microscopy," Annu. Rev. Biomed. Eng. **2**(1), 399–429 (2000).
24. D. R. Sandison, R. M. Williams, K. S. Wells, J. Strickler, and W. W. Webb, "Quantitative fluorescence confocal laser scanning microscopy (CLSM)," in *Handbook Of Biological Confocal Microscopy*, J. Pawley, ed. (Springer, 1995), Chap. 3, pp. 39–52.
25. D. W. Piston, "Imaging living cells and tissues by two-photon excitation microscopy," Trends Cell Biol. **9**(2), 66–69 (1999).
26. X. Hou and W. Cheng, "Single-molecule detection using continuous wave excitation of two-photon fluorescence," Opt. Lett. **36**(16), 3185–3187 (2011).
27. S. D. Smith, M. Shatsky, P. S. Cohen, R. Warnke, M. P. Link, and B. E. Glader, "Monoclonal antibody and enzymatic profiles of human malignant T-lymphoid cells and derived cell lines," Cancer Res. **44**(12 Pt 1), 5657–5660 (1984).
28. E. Schaeffer, R. Geleziunas, and W. C. Greene, "Human immunodeficiency virus type 1 Nef functions at the level of virus entry by enhancing cytoplasmic delivery of virions," J. Virol. **75**(6), 2993–3000 (2001).
29. W. Cheng, X. Hou, and F. Ye, "Use of tapered amplifier diode laser for biological-friendly high-resolution optical trapping," Opt. Lett. **35**(17), 2988–2990 (2010).
30. J. R. Moffitt, Y. R. Chemla, K. Aathavan, S. Grimes, P. J. Jardine, D. L. Anderson, and C. Bustamante, "Intersubunit coordination in a homomeric ring ATPase," Nature **457**(7228), 446–450 (2009).
31. N. Billinton and A. W. Knight, "Seeing the wood through the trees: a review of techniques for distinguishing green fluorescent protein from endogenous autofluorescence," Anal. Biochem. **291**(2), 175–197 (2001).
32. H. P. Lu, L. Xun, and X. S. Xie, "Single-molecule enzymatic dynamics," Science **282**(5395), 1877–1882 (1998).
33. W. E. Moerner and M. Orrit, "Illuminating single molecules in condensed matter," Science **283**(5408), 1670–1676 (1999).
34. N. J. Carter and R. A. Cross, "Mechanics of the kinesin step," Nature **435**(7040), 308–312 (2005).
35. P. J. Schuck, K. A. Willets, D. P. Fromm, R. J. Twieg, and W. E. Moerner, "A novel fluorophore for two-photon-excited single-molecule fluorescence," Chem. Phys. **318**(1-2), 7–11 (2005).
36. M. Drobizhev, N. S. Makarov, S. E. Tillo, T. E. Hughes, and A. Rebane, "Two-photon absorption properties of fluorescent proteins," Nat. Methods **8**(5), 393–399 (2011).
37. E. J. Peterman, S. Brasselet, and W. E. Moerner, "The fluorescence dynamics of single molecules of green fluorescent protein," J. Phys. Chem. A **103**(49), 10553–10560 (1999).
38. M. Drobizhev, S. Tillo, N. S. Makarov, T. E. Hughes, and A. Rebane, "Absolute two-photon absorption spectra and two-photon brightness of orange and red fluorescent proteins," J. Phys. Chem. B **113**(4), 855–859 (2009).

#157703 - $15.00 USD Received 7 Nov 2011; revised 15 Jan 2012; accepted 15 Jan 2012; published 18 Jan 2012

39. H. W. Ai, J. N. Henderson, S. J. Remington, and R. E. Campbell, "Directed evolution of a monomeric, bright and photostable version of Clavularia cyan fluorescent protein: structural characterization and applications in fluorescence imaging," Biochem. J. **400**(3), 531–540 (2006).
40. S. W. Hell, M. Booth, S. Wilms, C. M. Schnetter, A. K. Kirsch, D. J. Arndt-Jovin, and T. M. Jovin, "Two-photon near- and far-field fluorescence microscopy with continuous-wave excitation," Opt. Lett. **23**(15), 1238–1240 (1998).

1. Introduction

Fluorescence imaging at single-molecule level has become increasingly important in biophysical and cell biological studies [1]. The ability to visualize single molecules in real time allows direct observation of intermediate states that are often hidden in ensemble experiments [2]. The detection of these intermediates is often crucial in understanding these processes at molecular level [3]. To visualize single molecules in live cells, specific fluorophore labeling is required. Among the different types of fluorophores, green fluorescent protein (GFP) and its derivatives [4] can achieve high specificity of labeling through construction of fusion proteins with the target protein. The fusion protein usually has low perturbation to cell physiology and thus is a great choice for single-molecule detection in live cells. To image fluorescent proteins (FP) in a live cell at single-molecule level, it is essential to distinguish single FP fluorescence from the cell autofluorescence background. One strategy among others is to reduce the excitation volume. Several different imaging methods fall into this category, including TIRF [5], light sheet microscopy [6–8] and TPF [9,10]. Among these, TIRF uses the evanescent field to illuminate only a few hundred nanometers beyond interface and has been widely used to study plasma membrane and associated proteins at single-molecule level [11]. Recently, TIRF detection of single molecules has been widely used to measure stoichiometry of proteins in plasma membrane [12–16]. However, due to its limited penetration depth, TIRF is not feasible for imaging of fluorescent proteins that reside deep (>200 nm) inside the cell. To achieve single-molecule sensitivity inside eukaryotic cells that have larger cell body compared to bacterium, either light sheet microscopy or TPF is needed to suppress autofluorescence background. Recently, imaging of thick samples at single-molecule level using light sheet microscopy has been demonstrated [6–8]. However, to the best of our knowledge, TPF imaging of mammalian cells at single-molecule level has not been reported.

TPF involves the simultaneous absorption of two photons, the combined energy of which is sufficient to bring the fluorophore to an excited electronic state [17]. The probability for two-photon excitation is proportional to the square of photon density. Consequently TPF occurs most strongly near the optical focus within a limited volume of less than a femtoliter [18]. Due to the small localized excitation volume, both background fluorescence and photo damage are significantly reduced [9,19]. Thus, TPF has the great potential to achieve single-molecule detection in a live cell. Moreover, as TPF usually uses infrared laser for excitation, scattering and absorption are reduced compared to visible wavelength. It is therefore able to image thick samples with a good penetration depth [20–23]. As the excitation and emission wavelengths are well separated in TPF spectrum, background excitation light can be effectively removed by optical filters, which leads to a high signal to noise ratio. Due to the intrinsic three-dimensional (3D) resolution, there is no need for confocal aperture in the detection path, which increases the detection efficiency up to 20 fold [24] and greatly simplifies the alignment of optics [25].

Recently we have demonstrated optical detection of single GFP molecules using continuous-wave (CW) excitation of two-photon fluorescence [26]. We showed that EGFP that were immobilized on a coverslip surface could be detected at single-molecule level using TPF excited by a CW laser at 830 nm. Here we further test the possibility of single FP detection inside mammalian cells through TPF. Our results show that under TPF excitation, cell autofluorescence is low enough to permit detection of single FP molecules inside the cell. Both

#157703 - $15.00 USD Received 7 Nov 2011; revised 15 Jan 2012; accepted 15 Jan 2012; published 18 Jan 2012

single molecules of EGFP and mTFP1.0 can be detected, as indicated by their discrete stepwise photobleaching trajectories. We measured the on-time of single FPs before photobleaching. These results will be useful for future application of TPF in imaging of eukaryotic cells at single-molecule level.

2. Material and methods

2.1 Production of FP-labeled mammalian cells

To produce fluorescent cells for TPF imaging, we used two different methods. First, for cells that are difficult to transfect using conventional methods, we produced fluorescent cells by staining with FP solution after fixation of the cell using formaldehyde. We applied this method to sup-T1 cell, which is a human T cell line derived from a patient with T cell lymphoma [27]. Sup-T1 cells were cultured as suspension in RPMI 1640 with 10% fetal bovine serum (FBS). When cells reached a density of ~10^6 cells/mL, we collected the cells by centrifugation and fixed them in 4% formaldehyde solution for 15 min at room temperature. Cells were then washed once with PBS and resuspended in 0.5% Tween 20 solution to make cell membrane permeable. After incubation at room temperature for 30 min, cells were washed extensively and then resuspended in 100 μL PBS solution that contains 0.3 μM either EGFP (BioVision, Mountain View, CA) or mTFP1.0 (Allele Biotechnology, San Diego, CA). This staining process was carried out at room temperature for 2 hours with gently shaking, during which FPs spontaneously diffused into the interior of the fixed cells. The stained cells were then fixed one more time with 4% formaldehyde solution for 15 min to immobilize the FP, washed and resuspended in 50 μL PBS for TPF imaging. Second, for cells that can be conveniently transfected with plasmids, we use transfection to introduce FP labels. 293T cells were cultured in complete medium (90% Dulbecco's Modified Eagle Medium (DMEM) + 10% FBS) on a 12-well plate, and transiently transfected with a plasmid encoding EGFP-Vpr fusion protein [28] using calcium phosphate method. At 40 hours post transfection, medium was removed. Cells were washed gently with Dulbecco's Phosphate-Buffered Saline (DPBS), and detached from surface using Trypsin-EDTA. At 2 min after trypsin digestion, complete medium was added to stop the reaction. Cells were collected by centrifuge, washed once with Phosphate-Buffered Saline (PBS) and then fixed in 4% formaldehyde solution at room temperature for 15 min to immobilize the proteins inside the cell. After fixation, cells were washed once and finally resuspended in PBS for TPF imaging.

2.2 Cell immobilization on coverslip surface

The fixed cells were injected into a home-made microfluidic chamber (Fig. 1(a)) for TPF imaging. To facilitate the imaging of single FPs and multiple data collection, the injected cells

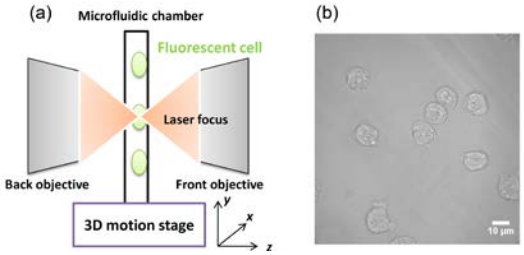

Fig. 1. (a) Experimental setup for single-molecule TPF imaging. Cells were immobilized onto the inner surface of the microfluidic chamber. The laser focus was positioned inside the cell. Lateral scanning of the chamber driven by a 3D motion stage (ESP300, Newport) allows searching of EGFP molecules inside the cell. (b) Sup-T1 cells attached non-specifically onto the coverslip surface.

#157703 - $15.00 USD Received 7 Nov 2011; revised 15 Jan 2012; accepted 15 Jan 2012; published 18 Jan 2012

were incubated inside the chamber for 30 min up to 1 hr, with the chamber lying flat. At the end of the incubation, multiple cells settled onto the coverslip surface by gravity and become immobilized non-specifically on the surface (Fig. 1(b)). We then install the chamber onto the microscope stage and start TPF imaging. The back objective in Fig. 1(a) is used to collect excitation laser for power measurement to ensure consistent laser power throughout imaging studies.

2.3 TPF imaging of single molecules inside fluorescent cells

Home-built optical tweezers [29] were used for TPF imaging with a CW tapered amplifier diode laser at 830 nm. We engaged the chamber to the front objective of optical tweezers, and adjusted the chamber axial position so that the laser focus falls inside the cell (Fig. 1(a)). We then scan the chamber laterally through a 3D motion controller (ESP300, Newport) to search for individual EGFP molecules and simultaneously use an EMCCD camera (Evolve, Photometrics) to collect the emitted fluorescence photons with an exposure time of 1 s. To optimize fluorescence readout on the camera from a single molecule, we defined a series of overlapping ROIs (regions of interest) to collect fluorescence photons in parallel. Each ROI has the same size of 5 pixels (1pixel = 270 nm × 270 nm) but differs in their locations by 1 pixel along x or y axis. The ROI with maximum fluorescence value was used for the subsequent measurement of that single molecule.

For all the imaging experiments, laser power was maintained at a stable level of 130.8 mW and exposure time was kept at 1 s unless otherwise noted. We used a custom-written Matlab program to analyze the fluorescence traces in terms of steps and dwells using a student t-test that was described previously [30]. From this analysis, fluorescence intensity and the on-time before photobleaching were obtained.

2.4 Fluorescence intensity as a function of excitation laser power

The details of this method have been described previously [26]. Briefly, we gradually decreased the laser power, and meanwhile recorded the fluorescence intensity from highly fluorescent spots within a transfected 293T cell using EMCCD. For TPF, fluorescence intensity has a quadratic dependence on excitation laser power. Therefore by fitting the logarithm of fluorescence intensity versus the logarithm of the laser power, the slope value indicates the number of photons absorbed to excite the fluorescence.

2.5 Simulation of single-molecule TPF bleaching trajectories with defined signal to noise ratio

Not every TPF trajectory we obtained showed photobleaching transitions that were close to ideal single molecules: some trajectories showed a slope transition instead of a clean and instantaneous off signal, the black trace in Fig. 3(a) below, for example. To better understand this phenomenon, we conducted simulation in Matlab. First, we created an ideal trace with an intensity value that was constant at 65 during the first 30 s and then dropped to 10 instantaneously due to photobleaching. The fluorescence intensity stayed at 10 thereafter. The experimental measurement of this process is always embedded with noise. To simulate the experimental trajectories, we created random Gaussian noise centered at 0, with a standard deviation (SD) of 15, and added this noise to the ideal trace. This standard deviation was chosen based on the experimentally observed noise in fluorescence intensities within a flat region. This process was repeated one hundred times and the resulting trajectories were compared to experimental data.

#157703 - $15.00 USD Received 7 Nov 2011; revised 15 Jan 2012; accepted 15 Jan 2012; published 18 Jan 2012

2.6 Monte Carlo simulation of single-molecule TPF intensity distribution

To better understand the distribution of the single-molecule fluorescence intensity from our measurements (Fig. 4(a) below), we conducted Monte Carlo simulations. The fluorescence intensity of a single molecule will depend on the location of the molecule within the excitation point spread function (PSF). We used a Gaussian function to approximate the shape of the PSF and simulated the TPF intensity F as follows, $F = A\exp(-r^2 / \omega_{xy}{}^2)$, where r is the radial distance of the single molecule away from center of the PSF, ω_{xy} is the 1/e width of the lateral intensity-squared profile [18], and A corresponds to the maximum fluorescence intensity when the molecule is located right at the center of the PSF. Under our excitation condition, ω_{xy} is estimated to be 160 nm [18]. We generated random values of r and calculated the fluorescence intensity F using Matlab. The F value can be regarded as the theoretical intensity of a single molecule. In reality however, there is always uncertainty derived from repeated measurements. We assumed a Gaussian distribution with a width d for this uncertainty. The resulting fluorescence value F_r was approximated as follows: $F_r = F + d \cdot R(0,1)$, where R(0,1) is a normally-distributed random number with mean at zero and standard deviation of 1. This random sampling was repeated to generate a total of 100,000 fluorescence values, which were further used to construct the histograms of fluorescence intensity (Fig. 6 below). Because it is difficult to assess the value of d from experiments due to the uncertainty in both molecular location and measurement errors, we systematically tested the effect of *d* on the resulting distributions of fluorescence intensities. We found that a *d* value from 5 to 10 can give rise to a centered peak distribution, which was close to the distribution we observed experimentally. When constructing the intensity histogram, we also set a threshold of 25 for detectable signal. Simulated intensity values lower than 25 were not counted in the histograms in order to account for the effect of experimental noise.

3. Results and discussion

3.1 Cell autofluorescence

To detect FP at single-molecule level inside mammalian cells, it is essential that the autofluorescence background from the cell content is lower than the fluorescence intensity from a single FP molecule under the same illumination conditions. Cellular autofluorescence is mainly contributed by metabolites and certain structural components inside the cell [31]. Its spectrum is usually quite broad, and overlaps the emission wavelength of GFP and its derivatives. To examine the cell autofluorescence under TPF conditions, we fixed freshly-cultured sup-T1 cells with formaldehyde and measured its autofluorescence by scanning laser focus throughout the entire cell. The results are shown in Fig. 2(a) as fluorescence intensity values along a single dimension of laser scanning. To compare cell autofluorescence with that of the solution background, each one-dimensional scan starts and ends with regions outside of a cell. The rough locations of cell boundaries are noted by arrows, which were indicated by bright field images of the cell being scanned. It is clear that the cell autofluorescence under TPF excitation is only minimally higher than the solution background, with an average intensity value of 10 across the entire cell. We have repeated this measurement for different sup-T1 cells and at different locations within the cell. The results are quantitatively similar, with an average TPF intensity of 10 within a single cell. However, the level of cell autofluorescence appears to depend on the cell-line studied, as the same measurement for 293T cells yielded an average fluorescence intensity of 30 compared to background. Of note, the autofluorescence background of a given location within a fixed cell increases very slowly with time. For example, the level of autofluorescence at a given location within a fixed sup-T1 cell increased to 37 (average from 7 independent measurements) after 10 min of constant laser

#157703 - $15.00 USD Received 7 Nov 2011; revised 15 Jan 2012; accepted 15 Jan 2012; published 18 Jan 2012

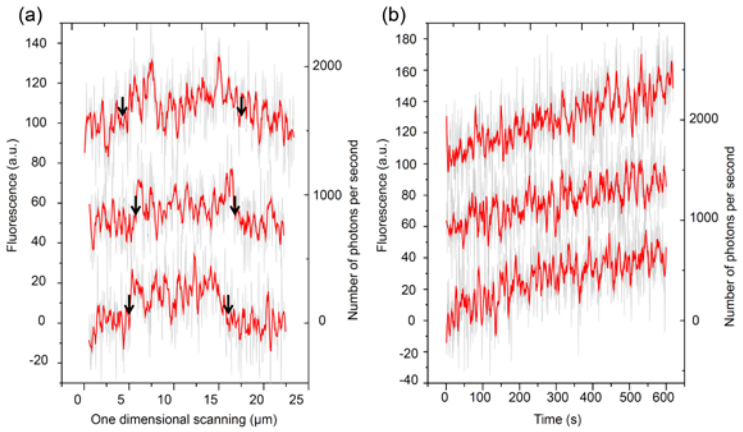

Fig. 2. (a) Three independent repeats of cell autofluorescence recorded during one-dimensional scanning of the laser focus across a fixed sup-T1 cell. Cell boundaries were marked by arrows. The gray traces were raw data at 50 nm step size while the red traces were boxcar averaged and decimated with a window size of 10. Traces were shifted along y-axis for clarity of display. (b) Under constant laser illumination, the autofluorescence from a single spot within a fixed sup-T1 cells increases very slowly with time. The gray traces were raw data at 1 Hz while the red traces were boxcar averaged and decimated with a window size of 10. Traces were shifted along y-axis for clarity of display.

illumination (Fig. 2(b)). This increasing trend is reproducible across different locations within a fixed sup-T1 or 293T cell. In contrast, the autofluorescence level for unfixed live cells does not show this time-dependence.

3.2 Single EGFP detection inside mammalian cells

To test the possibility of single FP detection within a mammalian cell using TPF, we produced fluorescent cells by either staining of fixed sup-T1 cells or transfection of 293T cells with EGFP-expressing plasmid. Sup-T1 cells are difficult to be transfected. Staining of the fixed cells bypasses the transfection step to achieve non-specific FP labeling. We found that the entire cell body could be stained by FP and the interior concentrations of FP could be easily controlled. Upon incubating these stained cells inside the microfluidic chamber, we focused the laser beam at the interior of the cell (Fig. 1(a)) and recorded fluorescence intensity over time at each focal spot. Figure 3 shows representative fluorescence trajectories from stained sup-T1 cells. In 70% cases, the fluorescence intensity stayed at a relatively constant value, and then bleached (Fig. 3(a)), which is the characteristic of the fluorescence emission from a single molecule followed by subsequent photobleaching [32,33]. Less frequently (30%), the fluorescence intensity underwent two (Fig. 3(b), (c)) steps of decrease before it bleached completely. Such fluorescence signals were never observed for unstained sup-T1 cells, suggesting that these fluorescence signals resulted from EGFP.

The caveat in imaging single EGFP molecules inside sup-T1 cells is that EGFP labels were introduced into the cells in a destructive manner: the cells were treated with detergent to allow EGFP diffuse to the interior of the cell. To test our ability of imaging single FPs within a cell close to biological conditions, we transfected 293T cells with EGFP-expressing plasmid, fixed the cells with formaldehyde and conducted imaging experiments. By doing so, the EGFP labels were introduced into cells through genetic expression, a condition that was extensively used in biological fluorescence imaging experiments. Upon expression, the EGFP molecules were distributed in both the cytoplasm and the nucleus [29], and thus provided a convenient marker

#157703 - $15.00 USD Received 7 Nov 2011; revised 15 Jan 2012; accepted 15 Jan 2012; published 18 Jan 2012

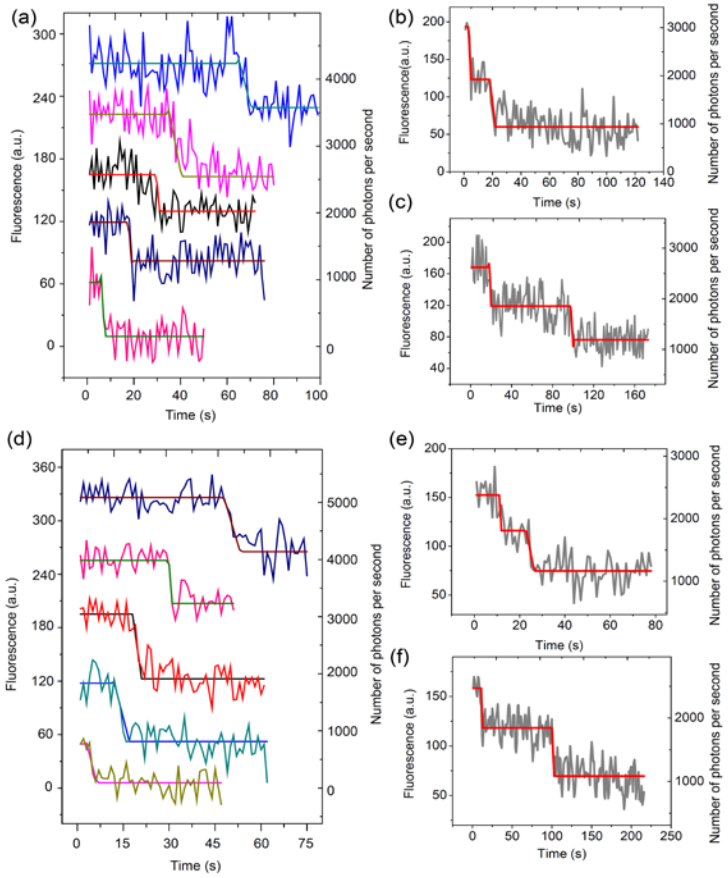

Fig. 3. Representative photobleaching trajectories recorded from EGFP inside sup-T1 and 293T cells. Experimental traces are shown together with corresponding traces simulated with a custom-written Matlab program. (a) Single-step photobleaching in supT-1 cells. Traces are arbitrarily shifted along y axis for clarity of display. (b, c) Two-step photobleaching in supT-1 cells. (d) Single-step photobleaching in 293T cells. Traces are arbitrarily shifted along y axis for clarity of display. (e, f) Two-step photobleaching in 293T cells.

for testing intracellular imaging. Indeed, EGFP molecules can be imaged inside 293T cells at single-molecule resolution, which was indicated by the stepwise photobleaching trajectories (Fig. 3(d)-(f)). These traces were collected in regions of low fluorescence intensity, so that single molecule can be clearly discerned.

3.3 Analysis of fluorescence intensity and dwell time

To quantitate these fluorescence signals collected from the interior of sup-T1 cells, we used a t-test analysis similar to previous methods [34] to automatically detect steps in these time trajectories of fluorescence, and obtained the histograms of fluorescence intensity and the on-time of fluorescence before photobleaching [26]. As shown in Fig. 4(a), the histogram of fluorescence intensity (results from 88 traces) shows a peaked distribution, which can be well described by a Gaussian function, with peak centered at 54.5 ± 1.0. This value is identical within error to the average TPF intensity of a single EGFP immobilized on coverslip surface, which is 55.0 ± 15.0 (20 traces) collected under identical instrument conditions. After consideration of our system collection efficiency (9%), this intensity value for a single EGPF

#157703 - $15.00 USD Received 7 Nov 2011; revised 15 Jan 2012; accepted 15 Jan 2012; published 18 Jan 2012

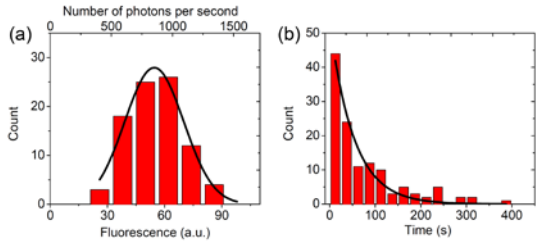

Fig. 4. Statistics of single EGFP fluorescence inside sup-T1 cell. (a) Histogram of fluorescence intensity (bin size of 12 a.u.). The black curve is fitted by a Gaussian function. (b) Histogram of fluorescence on-time before photobleaching (bin size of 20 s). The black curve is fitted by a single exponential decay.

molecule converts to ~9900 photons per second. Using the method developed by Schuck et al. [35], we further calculated the TPF cross section δ for EGFPs at 830 nm. Using a quantum yield of 0.76 for EGFP [36], this calculation yielded a δ value of 20.4 GM, which compared well with the recent report of 18.5 GM by Drobizhev et al. [36].

Figure 4(b) shows the distribution of the fluorescence on-time before photobleaching. Nonlinear least squares analysis shows that the data was best described by single exponential decay, with a time constant of 52.7 ± 5.2 s. This relaxation time constant is also identical within error to that of single EGFP on coverslip surface [26]. These results suggest that we can resolve the fluorescence of a single EGFP molecule inside sup-T1 cell. Each staircase in the fluorescence trajectories represents photobleaching of a single EGFP molecule. The time to photobleaching for individual EGFP molecules was dominated by a single rate-limiting event, in agreement with previous report [26,37]. About 5.2×10^5 photons were emitted by a single EGFP before photobleaching. Of note, the intensity value we reported here for a single EGFP is 67% higher than the value we reported previously for single EGFP on coverslip surface [26]. This difference is due to the optimization of ROI locations in current measurements (Materials and Methods), where a ROI that captured the maximum fluorescence intensity was used to record fluorescence.

3.4 Simulation of single-molecule TPF bleaching trajectories with defined signal to noise ratio

An ideal single-molecule photobleaching is expected to be a clean and discrete transition. However, ~10% of our traces collected show transitions with a slope (the black trace in Fig. 3(a)

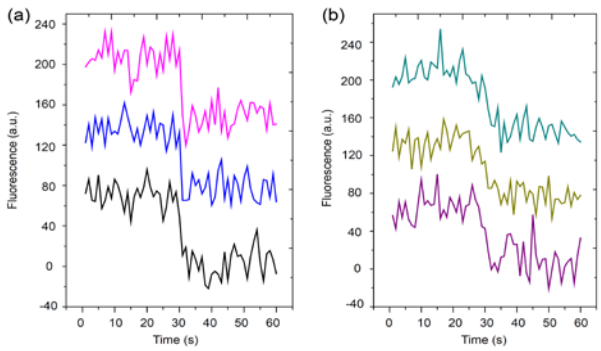

Fig. 5. Simulation of single-molecule bleaching trajectories. For an ideal transition that occurs at 30 s, ~90% traces show clear transitions in the presence of Gaussian noise, as shown in (a), while ~10% traces show transitions with a slope as shown in (b), which is similar to the black trace in Fig. 3(a).

#157703 - $15.00 USD Received 7 Nov 2011; revised 15 Jan 2012; accepted 15 Jan 2012; published 18 Jan 2012

for example). One possibility to account for this slope is the limited signal to noise ratio we have for these single-molecule measurements. The intensity of a single EGFP is around 54.5. The noise as we determined from fluorescence trajectories has a Gaussian distribution with a standard deviation ~15 (average from 7 traces). Thus, the signal to noise ratio (S/N) as we have for a single EGFP is ~3.6. To better understand these fluorescence trajectories, we thus simulated the single-molecule TPF bleaching trajectories with a defined S/N. As shown in Fig. 5, ~90% traces show clean steps (Fig. 5(a)) while ~10% show certain amount of delay (Fig. 5(b)). This simulation result is quantitatively consistent with our experimental observations and thus suggests that the delayed transitions in our traces may result from the limited S/N in these experiments.

3.5 Simulation of single-molecule TPF intensity distribution

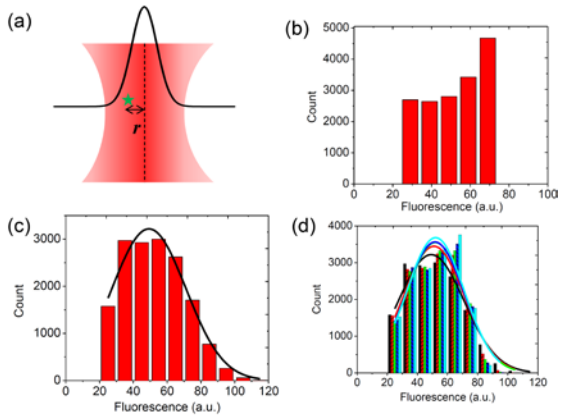

Fig. 6. (a) The TPF excitation volume has a Gaussian profile. '*r*' marks the radial distance of a fluorophore away from the center of the laser focus. (b) TPF intensity distribution in the absence of measurement noise for EGFP molecules that are randomly located within the excitation volume. (c) In the presence of uncertainties from repeated measurements (d = 10), the asymmetric distribution in (b) changes to become a Gaussian distribution, with peak centered around 50. (d) Increase in the experimental uncertainty d shifts the mean of the Gaussian profile to lower values (d value increases in the order: cyan 5, blue 5.5, green 6.2, red 7.1 and black10).

To better understand the shape of the fluorescence intensity distributions as we obtained in Fig. 4(a), we conducted Monte Carlo simulations. In the absence of measurement noise, the theoretical distribution of TPF intensity follows an asymmetric peak distribution (Fig. 6(b)), which is due to random distribution of single molecules within the TPF excitation volume. However, when we introduce uncertainties in the TPF intensity due to experimental measurement, this distribution becomes close to Gaussian (Fig. 6(c)), which corresponds to what we observed experimentally (Fig. 4(a)). With increasing measurement uncertainty d, the distribution shifts to Gaussian with lower peak values (Fig. 6(d)). These results suggest that the intensity distribution as we observed for single EGFP is a direct consequence of random locations of the molecules within the TPF excitation volume and experimental errors. Moreover, they also suggest that the maximum TPF intensity for a single molecule of EGFP is higher than the Gaussian peak value, which should be taken into account when estimating the brightness of the molecule.

#157703 - $15.00 USD Received 7 Nov 2011; revised 15 Jan 2012; accepted 15 Jan 2012; published 18 Jan 2012

3.6 The depth of single EGFP molecules within a stained sup-T1 cell

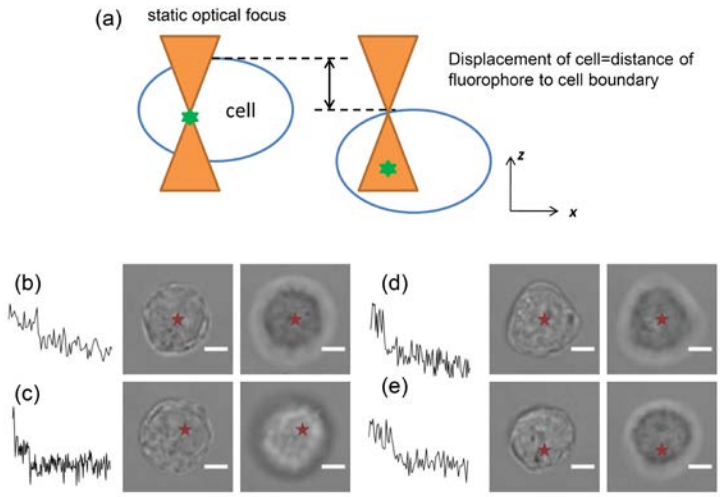

Fig. 7. Measurement of molecule depth inside a stained sup-T1 cell. (a) Cartoon representation of the experimental method. (b-e) Four independent examples of single EGFP molecules identified from these measurements. For each example, the stepwise bleaching of the single molecule TPF trajectory is shown on the left. The bright field image of the cell is shown in the middle, which also corresponds to the z-plane at which the single-molecule TPF signal was collected. The blurred cell images on the right shows the cell images after the chamber was moved away from the objective by a distance z so that the laser focus fell on the edge of the cell. Red star marks the position of the laser focus. The scale bar is 5 micron.

The advantage of TPF as compared to TIRF is the ability to penetrate deep samples due to intrinsic 3D resolution [20–23], which makes it possible to image single molecules deep inside a mammalian cell. To quantitate the depth of the single EGFP molecules that we can image, we conducted the following experiments: we scanned the laser focus within a stained sup-T1 cell; once a single EGFP molecule was identified through recording of stepwise photobleaching, we moved the microfluidic chamber in -z direction (Fig. 1(a)) until the cell boundary hit the laser focus. The TPF signal at this point drops to background and the distance that the chamber has travelled measures the depth of the single EGFP molecule (Fig. 7(a)).

Using this method, we have detected single EGFP molecules that were located at different depth within a sup-T1 cell, which are 8.1μm (Fig. 7(b)), 4.7 μm (Fig. 7(c)), 7.1 μm (Fig. 7(d)), and 6 μm (Fig. 7(e)), respectively. These results confirmed that indeed we could detect a single FP molecule deep inside a mammalian cell.

3.7 Fluorescence intensity as a function of excitation laser power

One would expect a quadratic dependence of fluorescence intensity on laser power if TPF occurs. To confirm that the fluorescence that we detected from EGFP molecules within 293T cells indeed resulted from TPF, we measured EGFP fluorescence intensity as a function of the excitation laser power. This measurement was done by focusing the laser on highly fluorescent spots inside the 293T cell, and measured the fluorescence intensity of EGFP as a function of laser power and plotted them on a logarithmic scale in Fig. 8. These plots from different spots within the cell are all well described by a linear relationship, with an average slope of 2.1, which confirmed that the fluorescence we detected from EGFP molecules indeed resulted from TPF. The slight deviation of this value from the theoretical slope of 2 can be explained by the fact of

#157703 - $15.00 USD Received 7 Nov 2011; revised 15 Jan 2012; accepted 15 Jan 2012; published 18 Jan 2012

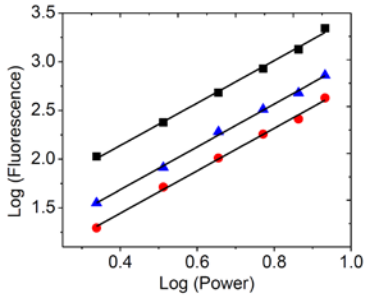

Fig. 8. EGFP fluorescence intensity as a function of laser power. Different symbols represent measurements from different spots within a 293T cell. Straight lines show linear fits in a double logarithmic scale, which give an average slope of 2.10 ± 0.01.

photobleaching. As we gradually decreased the laser power during this experiment, the fluorescence intensity measured at a new power setting will be lower than expectation due to photobleaching, and results in a slope that is higher than the theoretical value. Conversely, when this experiment was conducted in the order of increasing laser power, we obtained slope values that are 10-20% lower than 2, which further supports this interpretation.

3.8 Single mTFP1.0 detection inside stained sup-T1 cells

Under our current conditions, the 830 nm CW laser can excite TPF of EGFP that was detectable at single-molecule level inside a mammalian cell. However, the optimal wavelength of TPF excitation for GFP is 900 nm instead of 830 nm [38]. Although the current tapered amplifier diode laser has wavelength-tuning ability, it has a very limited range (810 – 845 nm) and therefore is not possible to work at 900 nm and thus limits the S/N of the detection. One potential solution to this problem is to use a variant of GFP that can be optimally excited at 830 nm. mTFP1.0 is such a FP that was derived from cyan fluorescent proteins through *in vitro* evolution [39]. Its two-photon cross section is about twofold higher than that of EGFP at 830 nm [36], and thus we expect this FP would give a higher S/N for single-molecule detection using 830 nm CW laser. To directly test this, we produced fluorescent sup-T1 cells that were stained with purified mTFP1.0 proteins (Allele Biotechnology, San Diego, CA), and conducted single-molecule imaging within sup-T1 cells under identical instrument conditions as those for EGFP. Figure 9(a) shows the representative traces of single mTFP1.0 photobleaching inside sup-T1 cells. By quantitating these fluorescence trajectories, we plotted the single-molecule TPF intensity distribution (Fig. 9(b), results from 189 traces), which shows a major peak centered at 111.9 ± 2.3. This intensity value is ~2 fold higher than that of a single EGFP molecule under identical conditions. Using a quantum yield of 0.84 for mTFP1.0 [36], the two-photon cross section we calculated for mTFP at 830 nm is 37.8 GM, which compared well with the recent report of ~37.0 GM by Drobizhev et al. [36]. Moreover, noise in single mTFP1.0 fluorescence trajectory is ~15 (average from 20 traces), so S/N is ~7.4 for single mTFP1.0 fluorescence, which is ~2 fold higher than that of EGFP. Figure 9(c) shows the distribution of the mTFP1.0 fluorescence on-time before photobleaching. Nonlinear least squares analysis shows that the data was best described by single exponential decay, with a time constant of 5.2 ± 0.4 s. This result suggests that the time to photobleaching for individual mTFP1.0 molecules was dominated by a single rate-limiting event, which is qualitatively consistent with that of EGFP. However, the rate of photobleaching is almost 10 fold faster than that of EGFP. Under one-photon excitation, the photostability of mTFP1 is 37% lower than that of EGFP [39]. The almost 10 fold difference in photobleaching rate as we observed here for two-photon excitation suggests that the mechanisms of photobleaching might be very different under two-photon

#157703 - $15.00 USD Received 7 Nov 2011; revised 15 Jan 2012; accepted 15 Jan 2012; published 18 Jan 2012

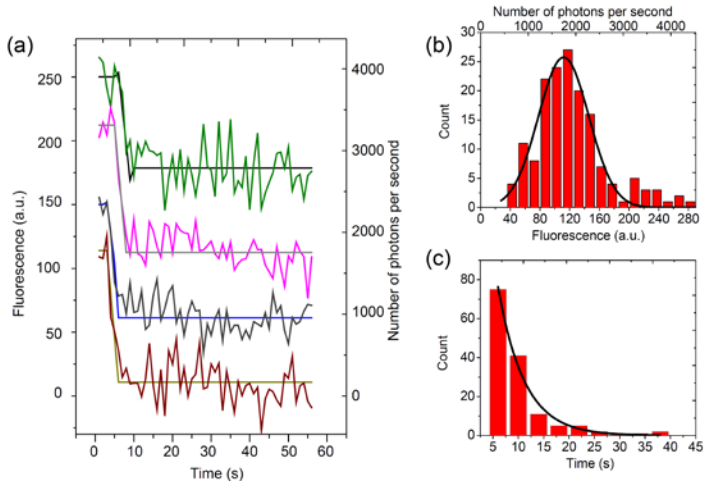

Fig. 9. (a) Time courses of single-molecule fluorescence of mTFP1.0 inside supT-1 cells. Experimental traces are shown together with corresponding traces simulated with a custom-written Matlab program. Traces are arbitrarily shifted along y axis for clarity of display. (b) Histogram of fluorescence intensity (bin size of 15 a.u.). The black curve is fitted by a Gaussian function. (c) Histogram of fluorescence on-time before photobleaching (bin size of 3 s). The black curve is fitted by a single exponential decay.

excitation conditions. Future research is needed to elucidate the possible mechanisms of this difference.

4. Conclusion

In this communication, we demonstrate that TPF can be used to detect single FP molecules inside mammalian cells, which adds TPF to the growing list of techniques that can resolve single-molecule fluorescence in the context of mammalian cells. The low autofluorescence background of a eukaryotic cell under two-photon excitation, and the bright TPF fluorescence signal from individual FP, together make it possible to image and quantitate eukaryotic cells at single-molecule level. Due to the intrinsic 3D resolution of TPF [9] and deep sample penetration [20,23], this imaging method is not limited to the surface of the cell, but can image proteins that are deep inside the cell. This technique has the huge potential to determine the stoichiometry of proteins that are located in the intracellular membranes. Stepwise photobleaching of single fluorescent molecules has become increasingly used to measure stoichiometry of membrane proteins in live cells [12–16]. The fluorescence intensity of a protein complex with one or more GFP labels drops in a stepwise fashion, and the number of steps reveals number of GFP tags and thus the stoichiometry of the complex. However, current technique relies on TIRF excitation to reduce background and resolve fluorescence at single-molecule level. It works for membrane proteins in the plasma membrane, as cells can be grown on poly-lysine coated coverslip and excitation is limited to the contact region between plasma membrane and the coverslip [15]. However, it will not work for proteins that reside in the intracellular membranes due to the limited penetration depth. In contrast, the ability of TPF to resolve single molecules inside mammalian cells makes this technique uniquely suited for stoichiometry measurement deep inside a cell beyond several microns, which is not feasible using TIRF. Lastly, ultrafast laser is typically used in TPF for biological applications. Compared to ultrafast lasers, several limitations exist for current approach: (1) although the current tapered amplifier diode laser has wavelength-tuning ability, it has a very limited range (810–845 nm) and therefore not as convenient as ultrafast lasers; and (2) CW laser is not

#157703 - $15.00 USD Received 7 Nov 2011; revised 15 Jan 2012; accepted 15 Jan 2012; published 18 Jan 2012

efficient in exciting molecules through two-photon process. To reach the same level of two-photon absorption rate and the same image brightness, 187-fold higher power is required for a CW laser than a typical pulsed laser (200 fs pulse width, 80 MHz repetition rate) [40]. This means that the sample needs to be compatible with a high laser power, or the kinetics of the process to be studied has to be slow so that one can use a long exposure time to reach decent image brightness. These drawbacks may limit the application of current approach to biological questions. However, the CW laser is cost-effective, usually takes a smaller footprint, and could thus be a great alternative when pulsed laser is not readily available.

Acknowledgments

We thank Cheng lab members, especially Rui Zhao for critical reading of the manuscript. This work is supported by NIH grant 1DP2OD008693-01, and also in part by the March of Dimes Foundation Research Grant No. 5-FY10-490. W. C. is a Basil O'Connor Starter Scholar of the March of Dimes Foundation. The following reagents were obtained through the AIDS Research and Reference Reagent Program, Division of AIDS, National Institute of Allergy and Infectious Diseases (NIAID), National Institutes of Health (NIH): Sup-T1 cell line from James Hoxie; pEGFP-Vpr from Warner C. Greene.

#157703 - $15.00 USD Received 7 Nov 2011; revised 15 Jan 2012; accepted 15 Jan 2012; published 18 Jan 2012